

# Supporting Information

## **Chemical Tuning of Specific Capacitance in Functionalized Fluorographene**

Eleni C. Vermisoglou, Petr Jakubec, Aristides Bakandritsos, Martin Pykal, Smita Talande, Vojtěch Kupka, Radek Zbořil, and Michal Otyepka\*

Regional Centre for Advanced Technologies and Materials, Department of Physical Chemistry, Faculty of Science, Palacký University Olomouc, 17. listopadu 1192/12, 771 46 Olomouc, Czech Republic

**Table S1.** Electrochemical properties of graphene materials functionalized covalently or non-covalently with small organic molecules that were used for supercapacitors (taken from the literature) and the respective properties of the present FG/Niso-24h covalent graphene derivative.

<i>3-electrode systems</i>	$C_{sp}$ F g <sup>-1</sup>	<i>Current density</i> A g <sup>-1</sup>	<i>Electrolyte</i>	<i>*Energy density</i> Wh kg <sup>-1</sup>	<i>Potential window</i> V	<i>Ref.</i>
AZ-SGH	350	1	1 M H <sub>2</sub> SO <sub>4</sub>		1.4	[1]
AQ/GF	396	1	1 M H <sub>2</sub> SO <sub>4</sub>		1.0	[2]
C/r-GO	310.8	0.5	6 M KOH		0.8	[3]
SFG	322.1	1	0.5 M H <sub>2</sub> SO <sub>4</sub>		1.2	[4]
G-CN	97	1	1 M Na <sub>2</sub> SO <sub>4</sub>		1.2	[5]
G-COOH	86	1	1 M Na <sub>2</sub> SO <sub>4</sub>		1.2	[5]
PYT-NH <sub>2</sub> /rGO	326.6	0.5	1 M H <sub>2</sub> SO <sub>4</sub>		0.8	[6]
<b>FG/Niso-24h</b>	<b>391</b>	<b>0.25</b>	<b>1 M Na<sub>2</sub>SO<sub>4</sub></b>		<b>0.7</b>	<b>This work</b>

<i>2-electrode systems</i>						
AZ-SGH	285.6	1	1 M H <sub>2</sub> SO <sub>4</sub>	18.2	1.4	[1]
TEA/rGO	200	0.2	1 M H <sub>2</sub> SO <sub>4</sub>	5.0	1.0	[7]
AQ/GF	32.3	1	1 M H <sub>2</sub> SO <sub>4</sub>	13.2	1.6	[2]
PYT-NH <sub>2</sub> /rGO//AC	77.2	0.5	1 M H <sub>2</sub> SO <sub>4</sub>	15.4	1.2	[6]
ODA-G	328.5	0.5	1 M Na <sub>2</sub> SO <sub>4</sub>	19.6	1.4	[8]
<b>FG/Niso-24h</b>	<b>105</b>	<b>0.25</b>	<b>1 M Na<sub>2</sub>SO<sub>4</sub></b>	<b>18.9</b>	<b>1.2</b>	<b>This work</b>

*\*Energy density results are quoted only in two-electrode systems that evaluate the actual supercapacitor performance.*

*Abbreviations:*

AZ-SGH: Self-assembled graphene hydrogels non-covalently functionalized with alizarin.

AQ/GF: Non-covalently functionalized graphene framework by anthraquinone.

C/r-GO: Carbon nanoparticles-anchored graphene nanosheets.

SFG: Spongy adenine-functionalized graphene.

G-CN: Cyanographene.

G-COOH: Graphene acid.

PYT-NH<sub>2</sub>/rGO: 2-aminopyrene-3, 4, 9, 10-tetraone (PYT-NH<sub>2</sub>), modified reduced graphene oxide (rGO).

PYT-NH<sub>2</sub>/rGO//AC: PYT-NH<sub>2</sub>/rGO with activated carbon (AC).

TEA/rGO: Triethanolamine functionalized reduced graphene oxide.

ODA-G: 4,4'-oxydianiline (ODA) pillared graphene

FG/Niso-24h: Fluorographene functionalized with 5-aminoisophthalic acid.

### Calculation of gravimetric capacitance (for three and two electrode systems), energy density and power density

The gravimetric capacitance for the three-electrode system was calculated from the measured discharge curve as follows:

$$C_m = \frac{I\Delta t}{m\Delta V} \quad (1)$$

where  $C_m$  is the gravimetric capacitance of the electrode ( $F\ g^{-1}$ ),  $I$  is the discharge current (A),  $t$  is the discharge time (s),  $\Delta V$  is the potential window and  $m$  is the mass of material deposited on the working electrode. The total gravimetric capacitance for the two-electrode cell was calculated as follows:

$$C_{m(\text{cell})} = \frac{4I\Delta t}{m\Delta V} \quad (2)$$

where  $C_{m(\text{cell})}$  is the gravimetric capacitance of the electrode ( $F\ g^{-1}$ ) and  $m$  is the total mass of material deposited on both electrodes. The energy density was estimated by using the formula  $E = CV_{\text{max}}^2/8$ . The power density, calculated from the constant current discharge curves and normalized by the total weight of the two electrodes  $m$  (g), was calculated according to the following equation<sup>[9]</sup>:

$$P = \frac{(V_{\text{max}} - V_{\text{drop}})^2}{4R_{\text{ESR}}m} \quad (3)$$

where  $R_{\text{ESR}}$  is the equivalent series resistance of the capacitor.

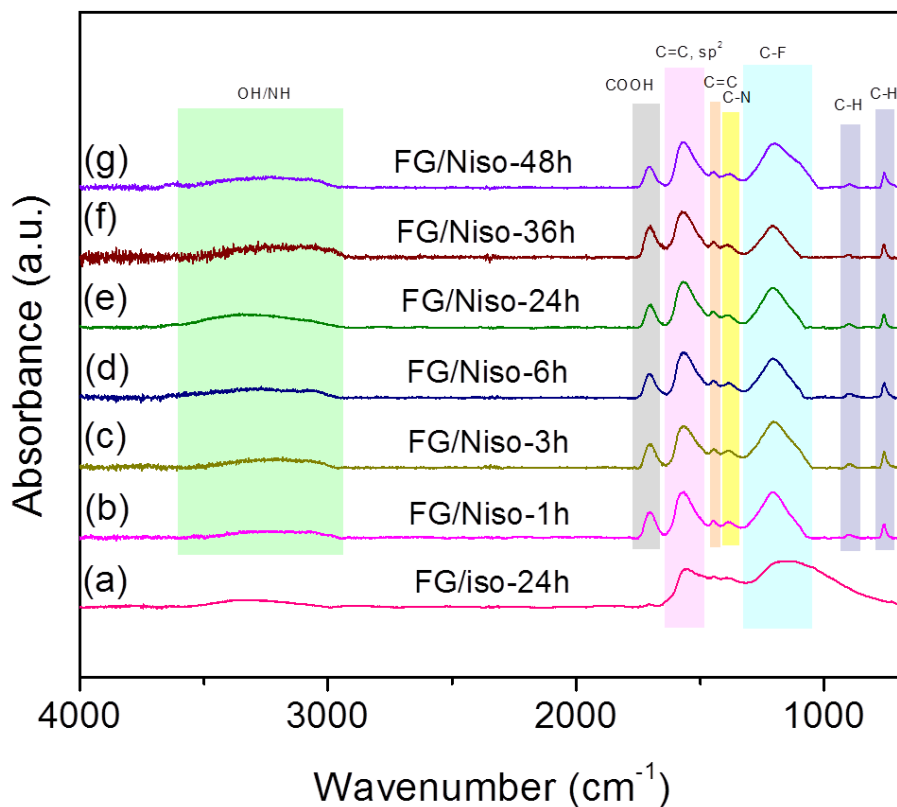


**Figure S1.** FTIR spectra of: (a) FG/iso-24h, (b) FG/Niso-1h, (c) FG/Niso-3h, (d) FG/Niso-6h, (e) FG/Niso-24h, (f) FG/Niso-36h, and (g) FG/Niso-48h samples. It can be seen that a doublet band in the region  $\sim 3400\text{-}3500\text{ cm}^{-1}$  attributed to a primary amine is absent in all the cases. Moreover, in the case of FG/iso-24h, the bands attributed to COOH, C=C, C-N, and C-H bending are absent.

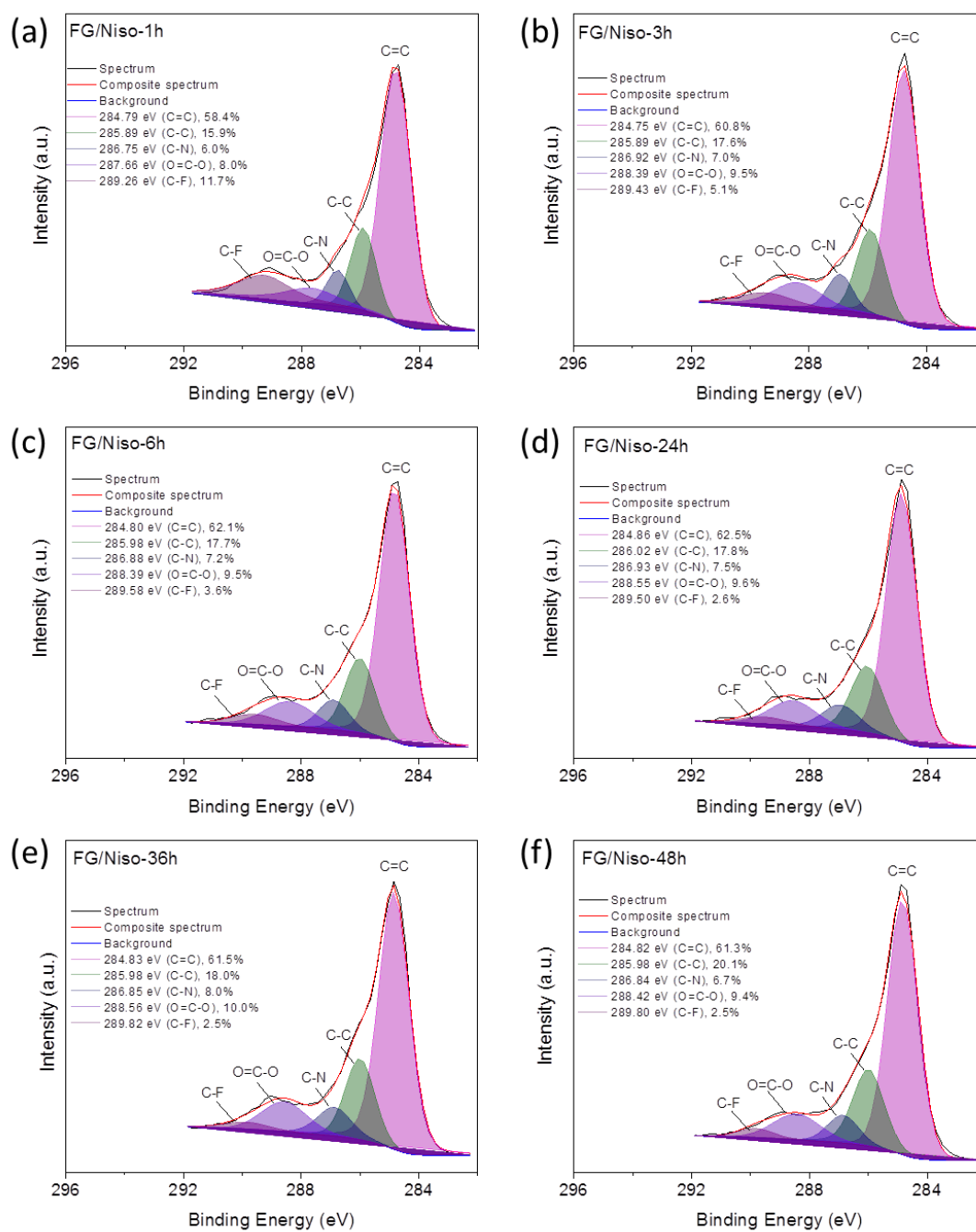


**Figure S2.** C1s XPS spectra of: (a) FG/Niso-1h, (b) FG/Niso-3h, (c) FG/Niso-6h, (d) FG/Niso-24h, (e) FG/Niso-36h and (f) FG/Niso-48h samples.

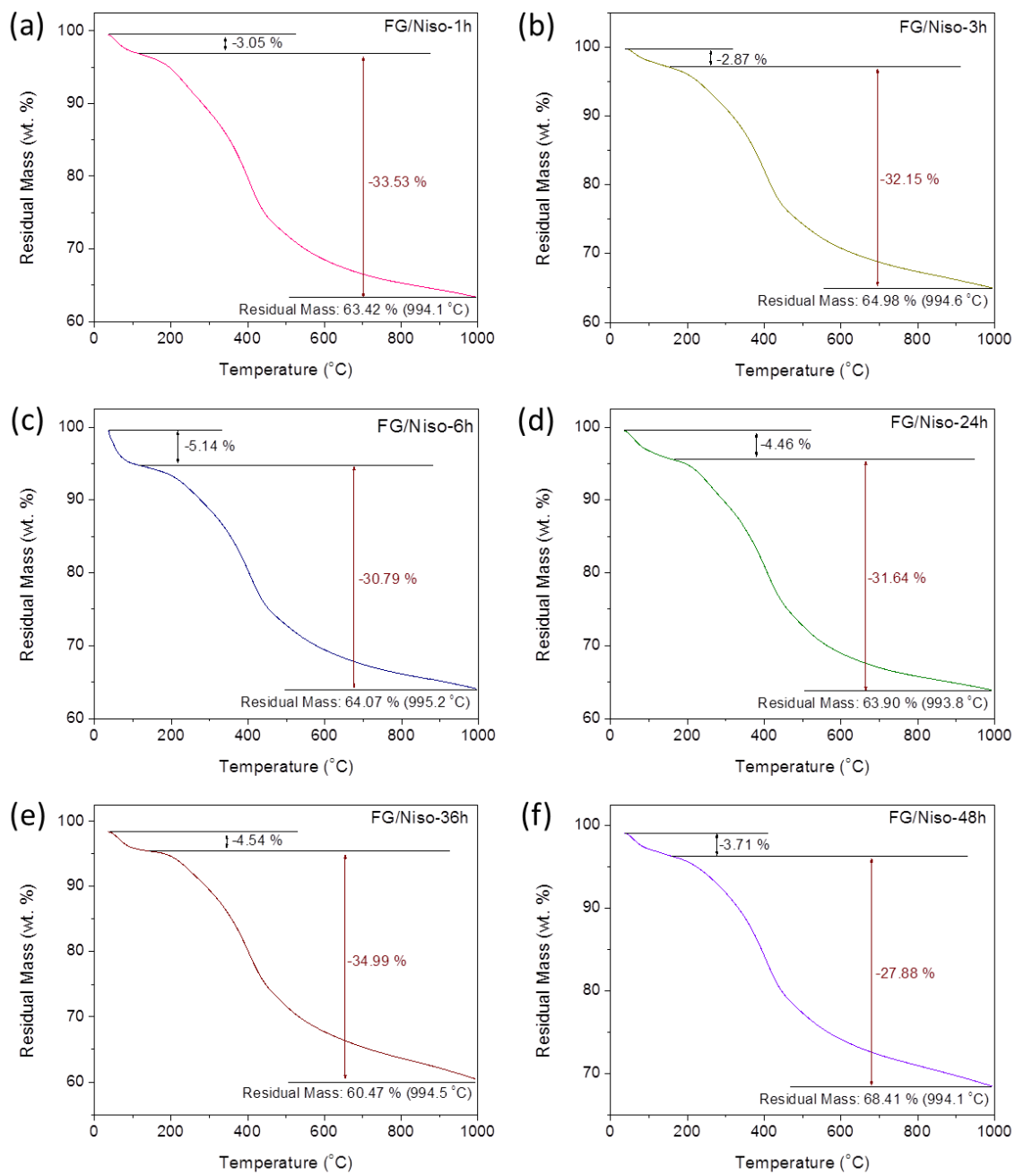


**Figure S3.** TGA analysis of: (a) FG/Niso-1h, (b) FG/Niso-3h, (c) FG/Niso-6h, (d) FG/Niso-24h, (e) FG/Niso-36h, and (f) FG/Niso-48h samples.

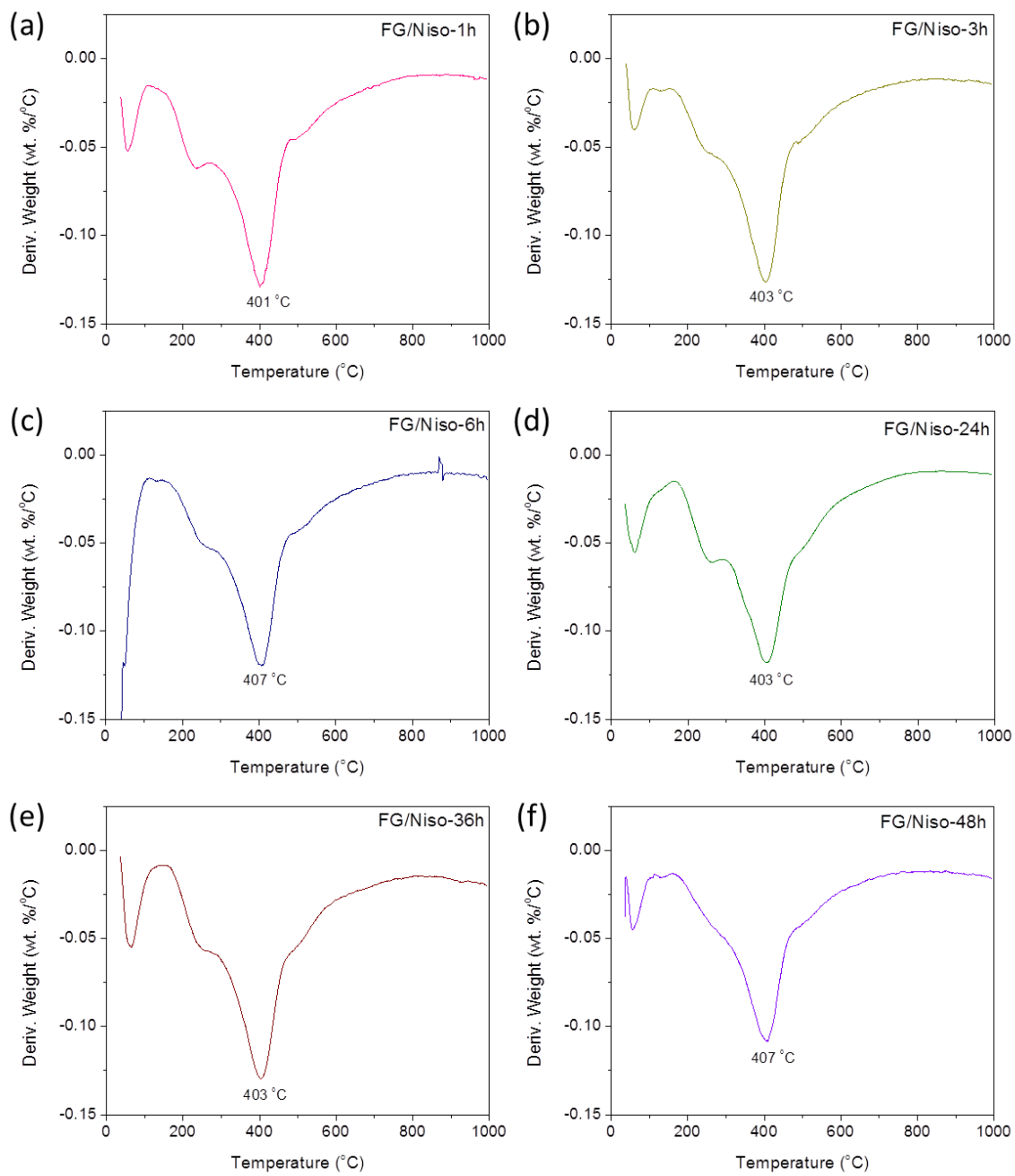


**Figure S4.** DTG analysis of: (a) FG/Niso-1h, (b) FG/Niso-3h, (c) FG/Niso-6h, (d) FG/Niso-24h, (e) FG/Niso-36h, and (f) FG/Niso-48h samples.

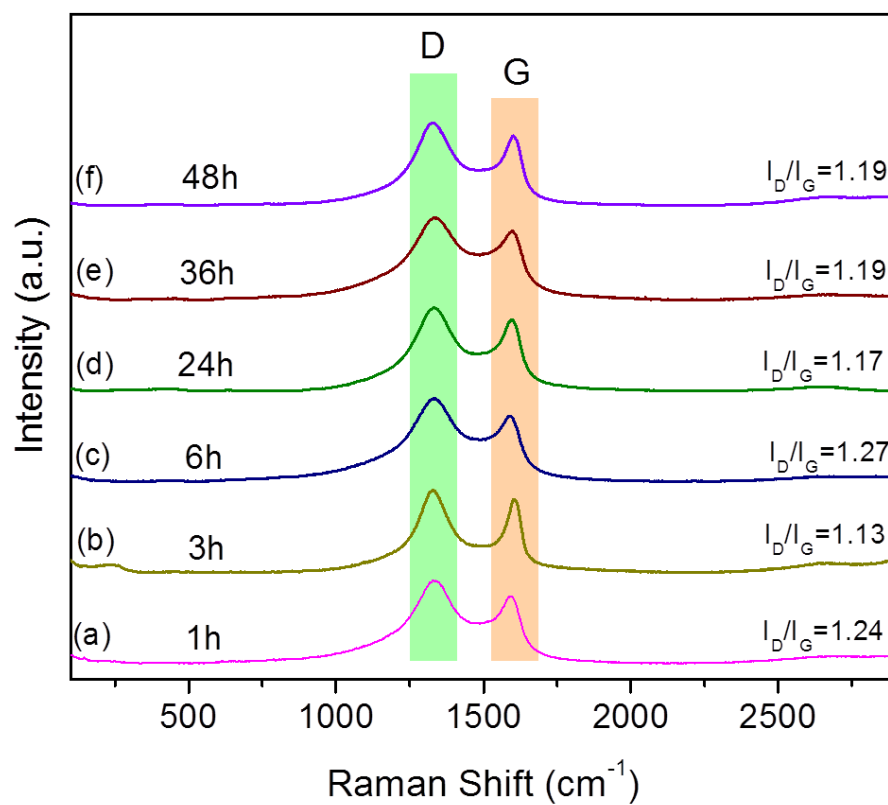


**Figure S5.** Raman spectra of (a) FG/Niso-1h, (b) FG/Niso-3h, (c) FG/Niso-6h, (d) FG/Niso-24h, (e) FG/Niso-36h, and (f) FG/Niso-48h samples and the corresponding intensity ratios  $I_D/I_G$ .

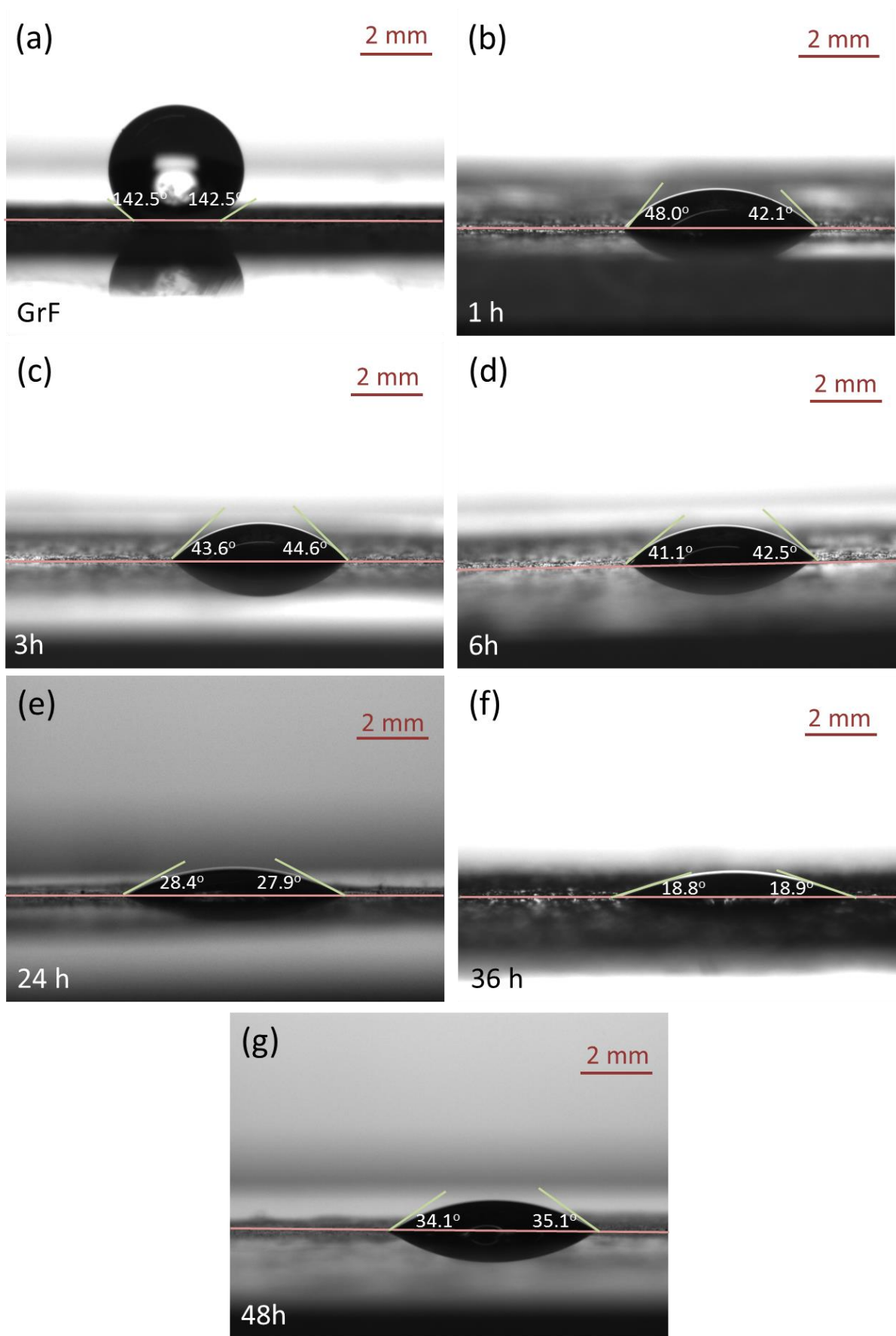


**Figure S6.** Water contact angle measurements of (a) GrF, (b) FG/Niso-1h, (c) FG/Niso-3h, (d) FG/Niso-6h, (e) FG/Niso-24h, (f) FG/Niso-36h and (g) FG/Niso-48h samples.

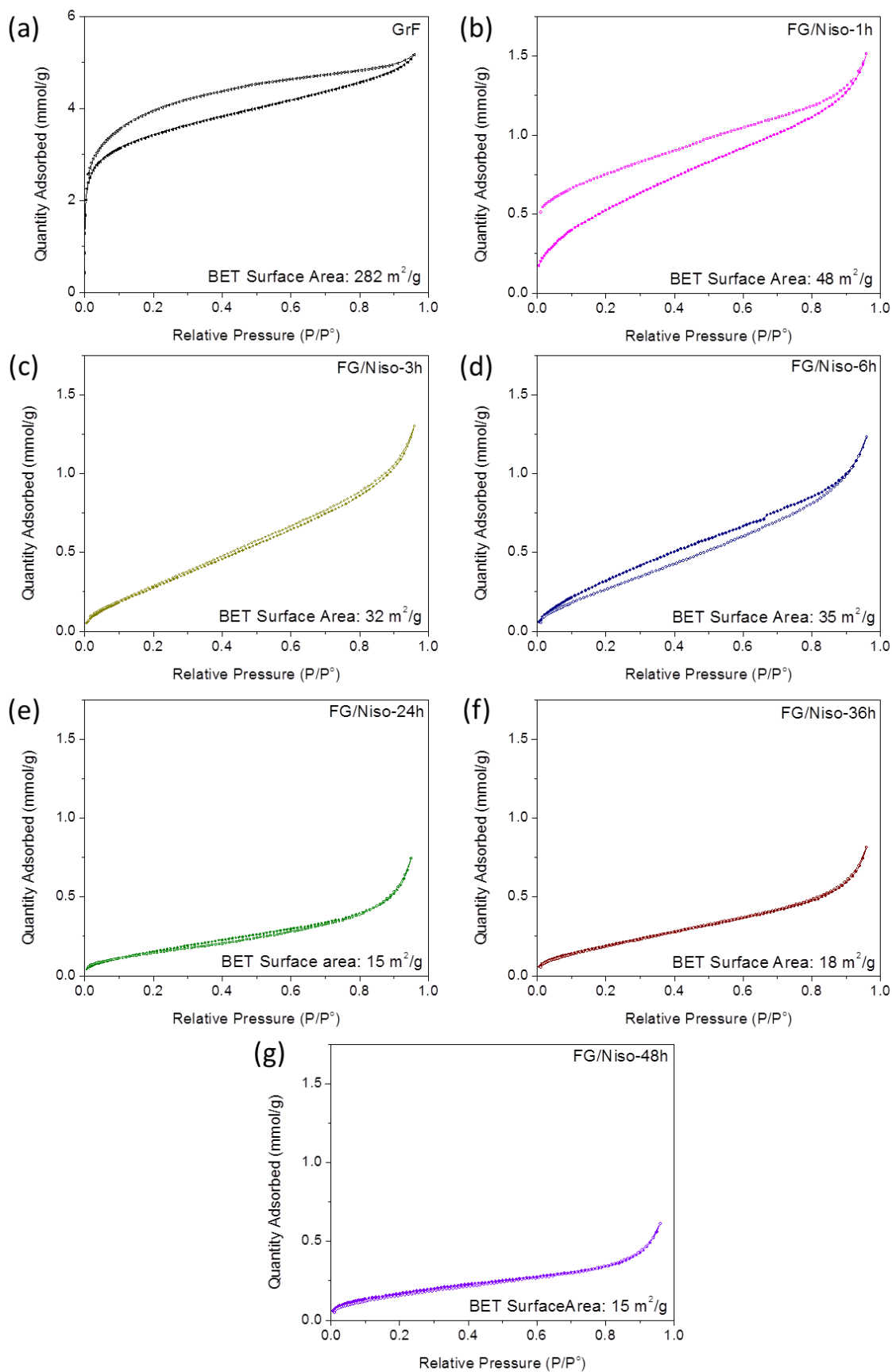


**Figure S7.**  $\text{N}_2$  adsorption/desorption isotherms obtained at  $-196^\circ\text{C}$  for (a) GrF, (b) FG/Niso-1h, (c) FG/Niso-3h, (d) FG/Niso-6h, (e) FG/Niso-24h, (f) FG/Niso-36h and (g) FG/Niso-48h samples.

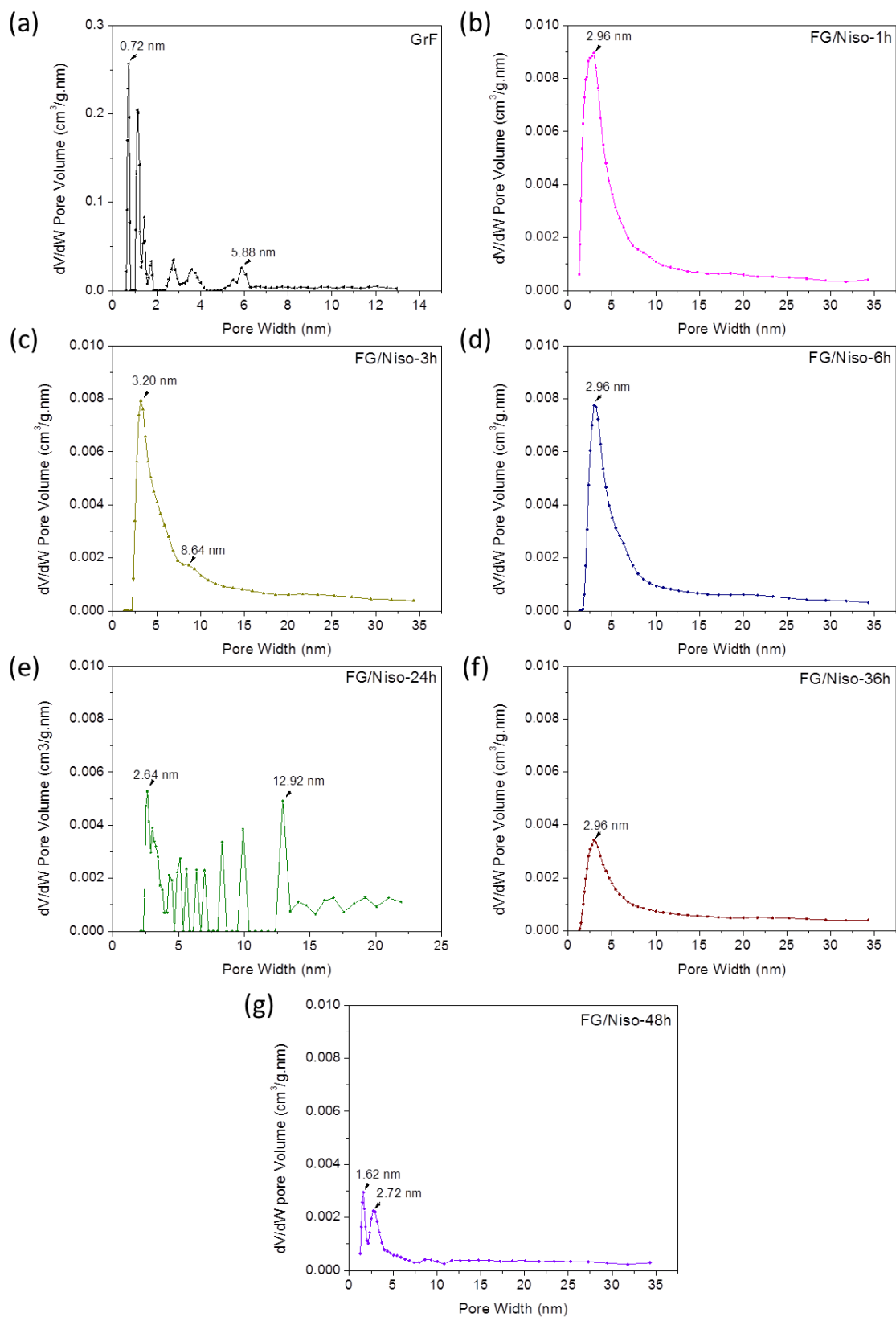


**Figure S8.** Pore size distributions derived using the DFT kernel for slit pores from the desorption branch of the isotherm for (a) GrF, (b) FGNiso-1h, (c) FG/Niso-3h, (d) FG/Niso-6h, (e) FG/Niso-24h, (f) FG/Niso-36h and (g) FG/Niso-48h samples.

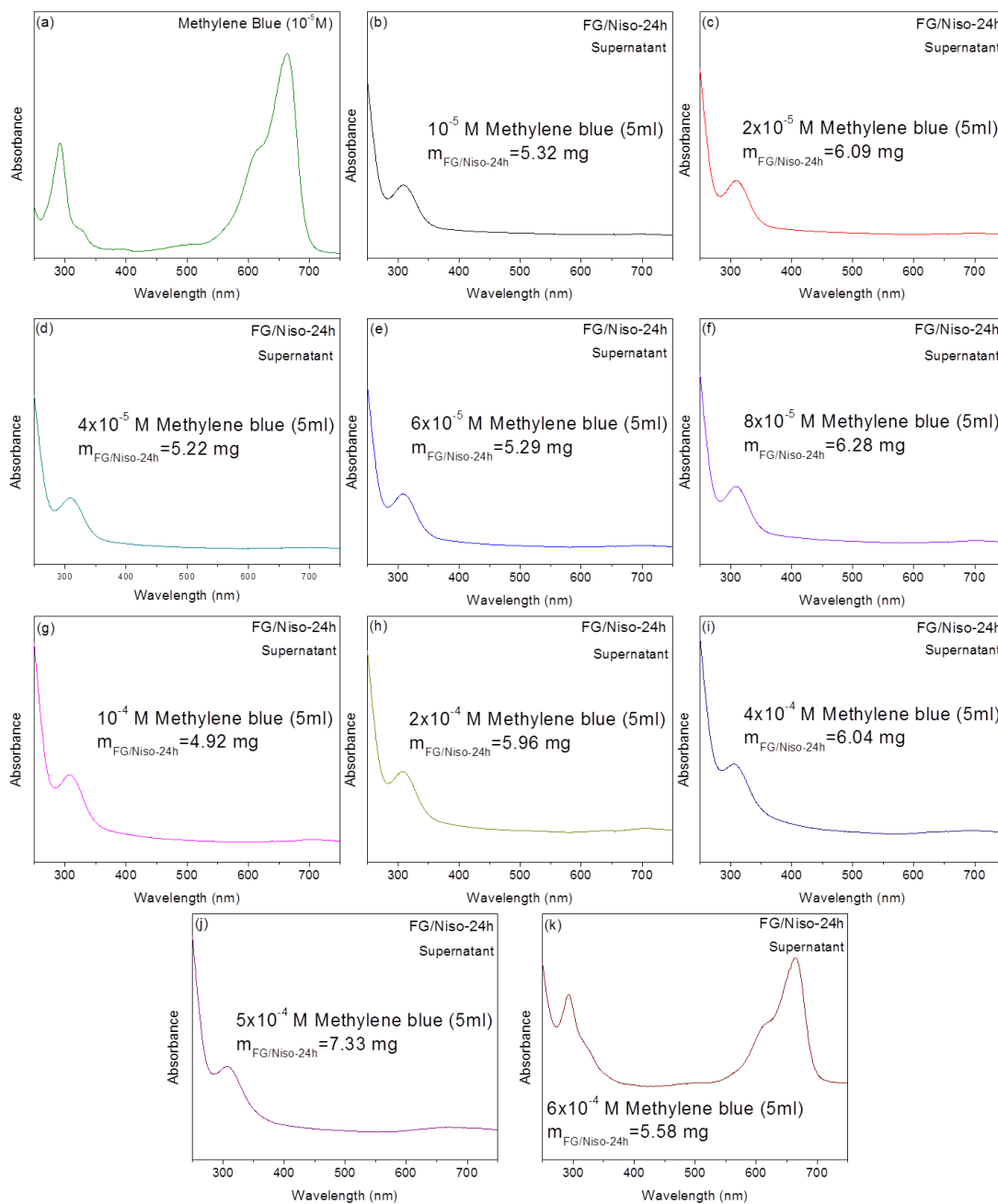


**Figure S9.** UV-vis absorption measurements of: (a) methylene blue  $10^{-5}$  M and (b-k) the supernatant liquid after the adsorption of methylene blue from aqueous solutions of different methylene blue concentrations by FG/Niso-24h sample. The initial methylene blue aqueous solutions (5ml) that were containing  $10 \mu\text{L}$  sodium borate buffer solution (pH~8.5) had concentrations ranging from  $10^{-5}$  M- $10^{-3}$  M. Till concentration  $5 \times 10^{-5}$  M, no methylene blue was traced in the supernatant. The peak at  $\sim 308\text{-}309$  nm is attributed to  $n \rightarrow \pi^*$  transition of the C=O band in the functionalized FG/Niso-24h. For the measurements a cuvette of 10 mm was used.

## Calculation of FG/Niso-24h loading in methylene blue and surface area from methylene blue adsorption measurements

The results from the UV-vis absorption measurements of the supernatant liquid after the adsorption of methylene blue from aqueous solutions of different concentrations by FG/Niso-24h sample (Figure S9), are summarized in the following adsorption curve:

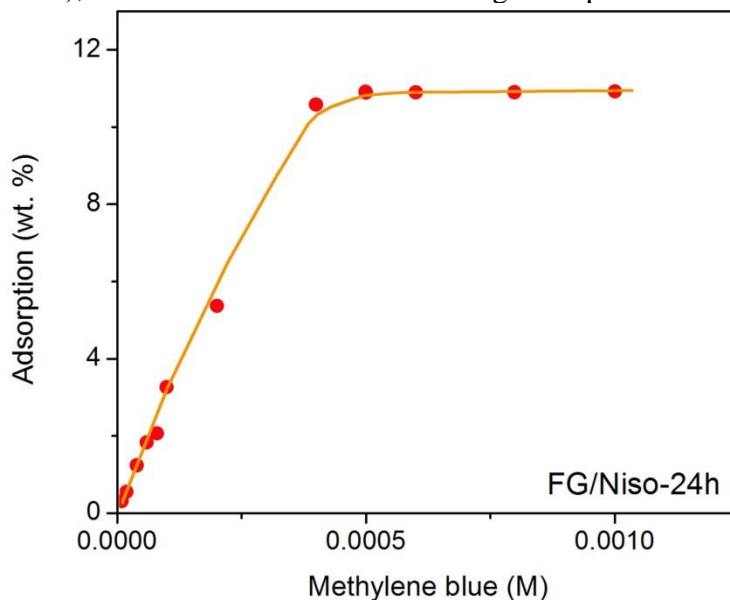


**Figure S10.** Methylene blue adsorption isotherm obtained at room temperature for FG/Niso-24h sample.

The maximum methylene blue adsorption by FG/Niso-24h was observed for concentration  $5 \times 10^{-4}$  M methylene blue. Above this concentration methylene blue was traced in the supernatant. 5 ml methylene blue solution  $5 \times 10^{-4}$  M contains  $2.5 \times 10^{-6}$  mol methylene blue i.e.  $8 \times 10^{-4}$  g methylene blue (Molecular weight of methylene blue: 319.85 g/mol). The amount of FG/Niso-24h that adsorbed this quantity of methylene blue was 7.33 mg i.e.  $7.33 \times 10^{-3}$  g. Thus the maximum wt. % loading of FG/Niso-24h in methylene blue is:  $(8 \times 10^{-4} \text{ g methylene blue} / 7.33 \times 10^{-3} \text{ g FG/Niso-24h}) \times 100 = 10.91 \text{ wt. \%}$ .

The specific surface area of FG/Niso-24h sample was calculated from the amount of methylene blue adsorbed by taking the area per adsorbed molecule as  $130 \text{ \AA}^2$ , which corresponds to the molecules lying flat on the FG/Niso-24h surfaces<sup>[10]</sup>. 1 mol methylene blue comprises of  $6.022 \times 10^{23}$  molecules methylene blue that each covers  $130 \text{ \AA}^2$ . Thus  $2.5 \times 10^{-6}$  mol methylene blue cover a surface:  $[(2.5 \times 10^{-6} \text{ mol methylene blue}) \times (6.022 \times 10^{23} \text{ molecules methylene blue/mol methylene blue}) \times (130 \times 10^{-20} \text{ m}^2/\text{molecule methylene blue})] / (0.00733 \text{ g FG/Niso-24h}) = 267 \text{ m}^2/\text{g}$ .

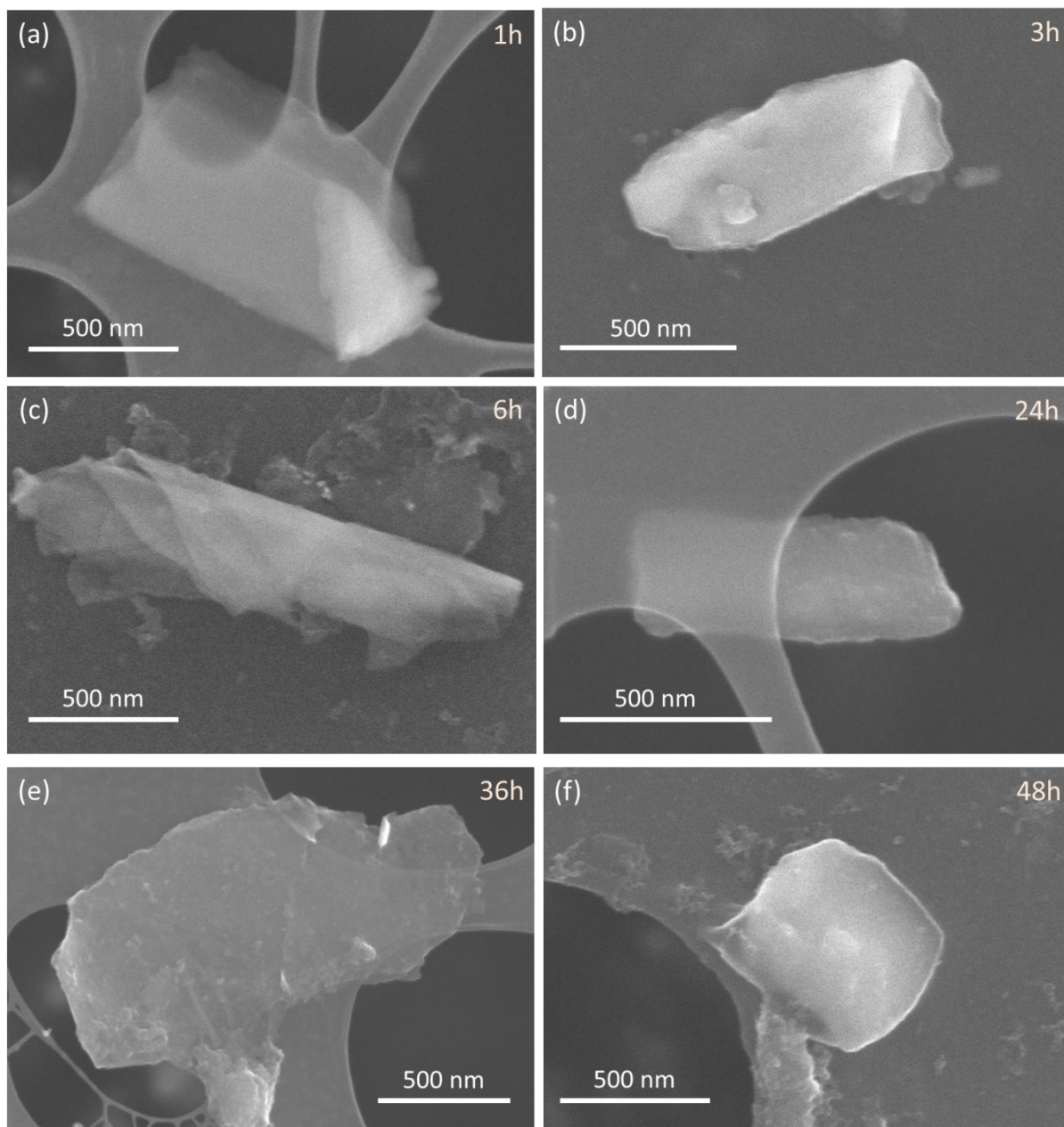


**Figure S11.** SEM images of: (a) FG/Niso-1h, (b) FG/Niso-3h, (c) FG/Niso-6h, (d) FG/Niso-24h, (e) FG/Niso-36h, and (f) FG/Niso-48h samples.

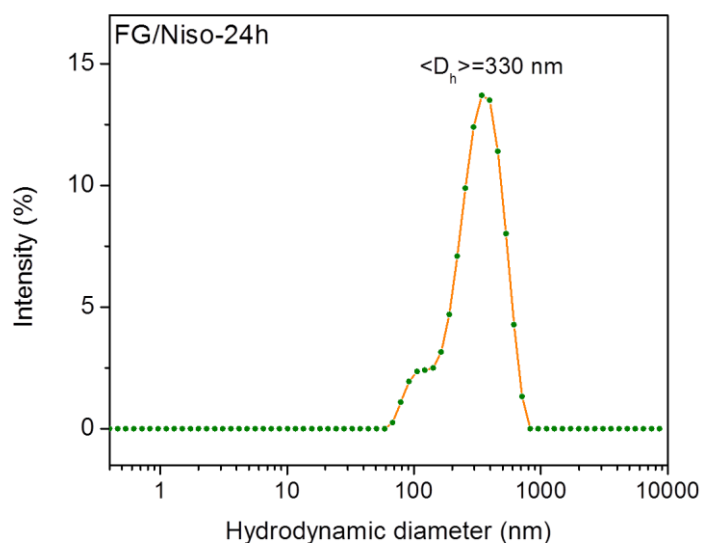


**Figure S12.** Intensity-weighted hydrodynamic diameter distribution of the FG/Niso-24h sample as obtained from dynamic laser-light scattering measurements, using a 0.2 wt% dispersion of the material.

The dynamic light scattering (DLS) footprint of the FG/Niso-24h colloids is shown in Figure S12, with a mean hydrodynamic diameter of 330 nm. This number should not be considered as an absolute size of the sheets. According to the principles of light scattering measurements, this is the size of a spherical particle, having the same diffusion coefficient as the studied colloids (i.e., a diffusion-based spherical equivalent). Nevertheless, the obtained result is a clear manifestation of the fine dispersion of the sheets and, roughly, of the dimensions of the colloidal entities therein. It should be also stressed that the size distribution is large, up to a size of 1000 nm, corroborating the findings from electron microscopy. The discotic shape of the basic structural units of FG/Niso-24h is also evident by the footprint of its hydrodynamic diameter distribution diagram, having a second maximum at ca 100 nm. Sheet-like materials, such as laponite with 1 nm sheet thickness,<sup>[11]</sup> respond as having two different diffusion coefficients, one corresponding to smaller and another to larger particles. This pattern is interpreted on the basis of the nanodiscs' orientation in relation to the vector of velocity. Those particles moving with their large fore-front against the solvent display small diffusion rates, while those (or when during the measurement) particles moving with their thin edges against the solvent exhibit higher diffusion rates (i.e., a smaller apparent hydrodynamic diameter). Overall, the DLS results confirm a material with sheet-like structure, and approximate span of flake size from 150 nm to 1  $\mu\text{m}$ .

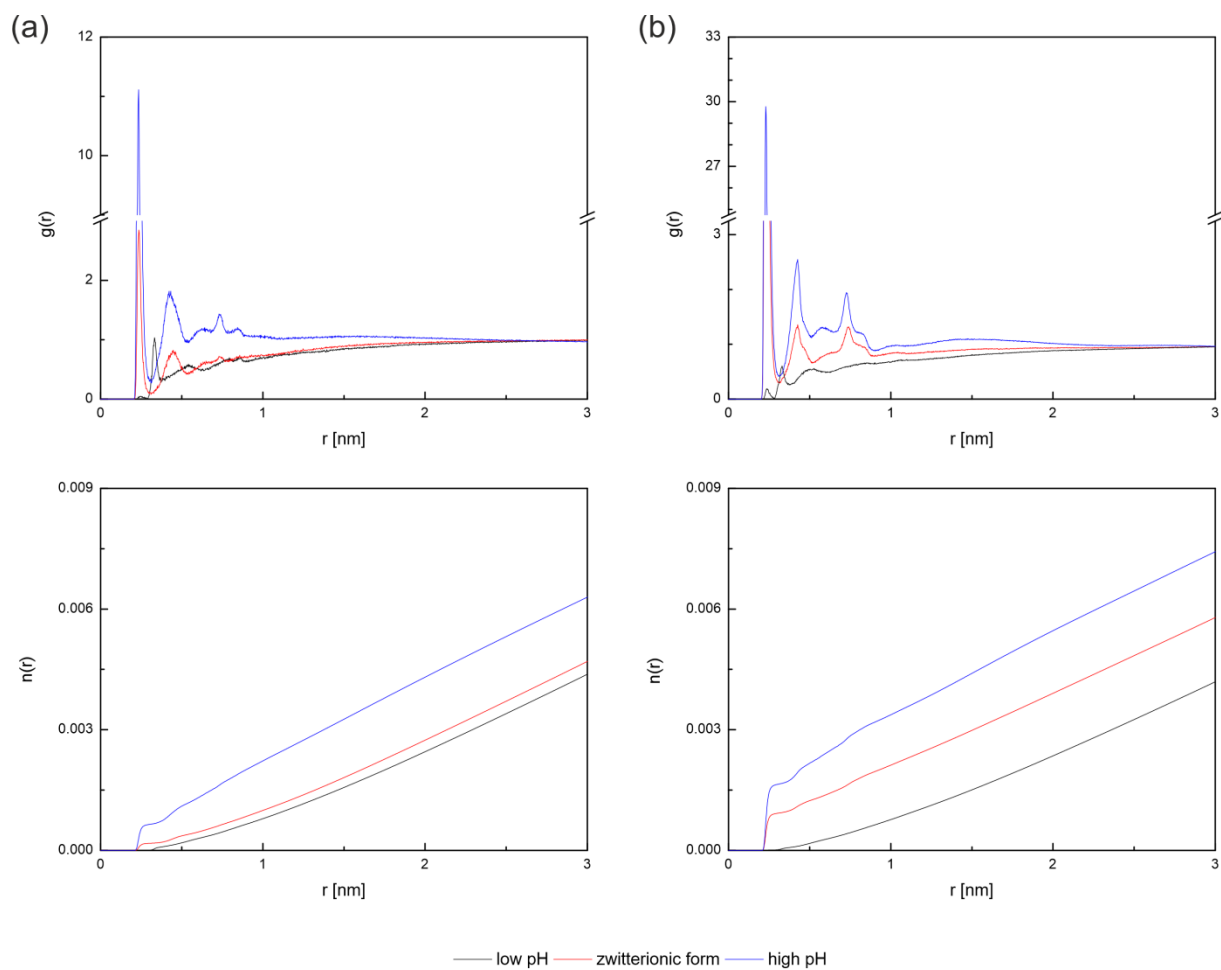


**Figure S13.** Radial distribution functions  $g(r)$  of ions ( $\text{Na}^+$  and  $\text{Cl}^-$ ) around titratable groups of (a) single- and (b) three-layered Niso derivative at different pH (top) and their integral values  $n(r)$  (bottom). Black line stands for structure at low pH, red line for the zwitterionic form and blue line represents Niso derivative at high pH.

### Calculation of functionalization degree (FD) from XPS and TGA results

*Example for FG/Niso-24h:* At ~1000 °C, the total mass loss is 31.64 wt. % and the residual mass - if we take into consideration the initial removal of water (4.46 wt. %) - is 63.90 wt. % containing only carbonaceous graphene material (*Figure S3d*). The elemental composition of FG/Niso-24h derived from XPS analysis (Table 1) corresponds to a formula  $C_{77.6}N_{5.8}O_{14.7}F_{1.9}$  with a molecular weight 1284.55 g/mol and a fluorine weight percentage of 2.81 wt. %. In TGA of FG/Niso-24h (Figures 2a, S3(d)), the mass loss of 31.64 wt. % is assigned both to functionalities (*fn*: 5-aminoisophthalic acid, molecular weight 181.15 g/mol) and fluorine. Thus, by subtracting the fluorine weight percentage (2.81 wt. %) from the total percentage i.e. 31.64 wt. %, it is found that 28.83 wt. % corresponds to *fn*. So, (63.90 g *graph*)/(12.0107 g *carbon/atom*) correspond to (28.83 g *fn*)/(181.15 g *fn/mol*) which gives in 33.43 *carbon atoms* / 1 mol *fn* resulting in 2.99~3.0 mol *fn*/100 graphene carbon atoms. Thus, the FD is ~3.0. Similarly, the FDs for all the samples can be calculated.

### References

1. An, N.; An, Y.; Hu, Z.; Guo B.; Yang, Y.; Lei, Z. Graphene hydrogels non-covalently functionalized with alizarin: an ideal electrode material for symmetric supercapacitors *J. Mater. Chem. A* **2015**, *3*, 22239-22246.
2. An, N.; Zhang, F.; Hu, Z.; Li, Z.; Li, L.; Yang, Y.; Guo, B.; Lei, Z. Non-covalently functionalizing a graphene framework by anthraquinone for high-rate electrochemical energy storage *RSC Adv.* **2015**, *5*, 23942-23951.
3. Huang, Y.; Gao, A.; Song, X.; Shu, D.; Yi, F.; Zhong, J.; Zeng, R.; Zhao, S.; Meng, T. Supramolecule-Inspired Fabrication of Carbon Nanoparticles In Situ Anchored Graphene Nanosheets Material for High-Performance Supercapacitors *ACS Appl. Mater. Interfaces* **2016**, *8*, 26775-26782.
4. El-Gendy, D. M.; Abdel Ghany, N. A.; Foad El Sherbini, E. E.; Allam, N. K. Adenine-functionalized Spongy Graphene for Green and High-Performance Supercapacitors *Scientific Reports* **2017**, *7*, 43104.
5. Cheong, Y. H.; Nasir, M. Z.; Bakandritsos, A.; Pykal, M.; Jakubec, P.; Zbořil, R.; Otyepka, M., Pumera, M. Cyanographene and Graphene Acid: The Functional Group of Graphene Derivative Determines the Application in Electrochemical Sensing and Capacitors *Chem. Electro. Chem.* **2018**, <https://doi.org/10.1002/celec.201800675>.
6. Shi, J.; Zhao, Z.; Wu, J.; Yu, Y.; Peng, Z.; Li, B.; Liu, Y.; Kang, H.; Liu, Z. Synthesis of Aminopyrene-tetraone-Modified Reduced Graphene Oxide as an Electrode Material for High-Performance Supercapacitors *ACS Sustainable Chem. Eng.* **2018**, *6*, 4729-4738.
7. Song, B.; Sizemore, C.; Li, L.; Huang, X.; Lin, Z.; Moon, K.; Wong, C. P. Triethanolamine functionalized graphene-based composites for high performance supercapacitors *J. Mater. Chem. A* **2015**, *3*, 21789-21796.
8. Zhao F.G.; Kong, Y. T.; Pan B.; Hu C. M.; Zuo B.; Dong X.; Li B.; Li W.S. *In situ* tunable pillaring of compact and high density graphite fluoride with pseudocapacitive diamines for supercapacitors with combined predominance in gravimetric and volumetric performances *J. Mater. Chem. A* **2019**, *7*, 3353-3365
9. Zhao X.; Zhang L.; Murali S.; Stoller M. D.; Zhang Q.; Zhu Y.; Ruoff R. S. Incorporation of manganese dioxide within ultraporous activated graphene for high-performance electrochemical capacitors *ACS Nano* **2012**, *6*, 5404-5412.
10. Hang T. P.; Brindley G. W. Methylene blue absorption by clay minerals. Determination of surface areas and cation exchange capacities. (Clay-organic studies XVIII) *Clays and Clay Minerals* **1970**, *18*, 203-212.
11. Tzitzios V.; Basina G.; Bakandritsos A.; Hadjipanayis C.G; Mao H.; Niarchos D.; Hadjipanayis G. C.; Tucek J.; Zboril R. Immobilization of magnetic iron oxide nanoparticles on laponite discs – an easy way to biocompatible ferrofluids and ferrogels *J. Mater. Chem.* **2010**, *20*, 5418-5428.